Andreev scattering at a rough surface of ^{3}He-B

Weiyi Zhang
Research Institute for Theoretical Physics, University of Helsinki, Siltavuorenpenger 20, SF-00170 Helsinki 17, Finland

J. Kurkijärvi
Institute of Physics, Åbo Akademi, Porthansgatan 3, SF-20500 Åbo, Finland

D. Rainer
Physikalisches Institut der Universität Bayreuth, D-8580 Bayreuth, Federal Republic of Germany

E. V. Thuneberg
Laboratory of Atomic and Solid State Physics, Cornell University, Clark Hall, Ithaca, New York 14855-2501
(Received 24 August 1987)

Quasiclassical methods are used to study the reflection of wave packets at diffusely scattering surfaces of ^{3}He. In addition to conversion into nonmagnetic and magnetic holes and partial specular reflection into nonmagnetic and magnetic wave packets, diffuse background scattering of nonmagnetic and magnetic particles and holes into all directions is found. The calculations are based on the self-consistently computed order parameter in the vicinity of the wall.

I. INTRODUCTION

The microscopic dynamics of superfluid ^{3}He-B is contained in the solutions of the quasiclassical 4×4 matrix equation for the Keldysh Green's function. The matrix space arises from the particle-hole and the spin degrees of freedom.[1] Half of the 16 modes are propagating excitations and the other half are so-called Tomasch interferences. One can further separate the propagating modes into particlelike or holelike according to whether their group velocities are parallel or antiparallel to the wave vector. Among the particlelike propagating excitations, one is nonmagnetic and the other three are magnetic. There are also the exact holelike equivalents. Finally the Tomasch solutions are superpositions of particlelike and holelike excitations. This makes for a rich variety of possibilities.

The complete dynamics of superfluid ^{3}He-B features collective excitations in addition to the microscopic modes. Quasiparticle excitations and collective excitations are coupled in general. In this paper we assume a low density of quasiparticles and, hence, do not explicitly consider collective excitations.

Rapid variations in the order parameter lead to spectacular behavior of propagating quasiparticle excitations.[2] When a quasiparticle, originally on its way in equilibrium with the surrounding order parameter, suddenly finds itself completely out of tune with what it sees around it, it stops on its tracks, converts into a hole and turns back (Andreev scattering) or turns into a different kind of excitation (branch conversion process) flying either in the original (transmitted) direction or precisely against it (reflected direction). The walls of a container are the obvious places where quasiparticles meet such a fate. There the order parameter of a p-wave superfluid is known to become partly or completely suppressed[3,4] which provides for the requisite rapid variation of the order parameter.

The scattering problem of quasiparticles of a superfluid phase off a rough surface is of some theoretical interest. It can be handled by the quasiclassical approach[5] where it looks, at a first glance, like an overdetermined problem. Out of a single wave vector direction of incoming particles, the diffusely scattering surface sends excitations into random directions in space but obviously only of those kinds which propagate back into the fluid from the surface. This leads to a larger number of conditions to be satisfied by the solution of the equation of motion for the relevant Green's function than there are degrees of freedom available. It turns out, almost miraculously, that the normalization condition of the theory eliminates just those solutions which would violate ones intuition and leaves behind exactly the correct number of coefficients to be determined.

In principle, Andreev scattering or branch conversion processes can be measured directly.[6] When they occur at a wall, they also have important indirect implications on the boundary condition of superfluid flow.[7,8] The usual boundary condition of hydrodynamics requires stationarity of the fluid on a surface. If the mean free path of the momentum-carrying particles becomes so long, however, that full local equilibrium reigns no more, a first remedy is a more general boundary condition[9] where the velocity is required to vanish only at a slip length's distance outside the surface. One understands easily that a quasiparticle, which becomes Andreev reflected, exchanges very little momentum with the wall. It, therefore, should reduce the diffusivity of scattering at a boundary and enhance the required slip correction to viscosity measurements.[10] At a wall which scatters quasiparticles specu-

larly, Andreev reflection and the branch conversion processes have been studied in detail by Kieselmann and Rainer.[1]

Having previously computed the order parameter near a diffusely scattering wall,[11] here we report computations on Andreev scattering and branch conversion amplitudes, including scattering into diffuse background states of continuous wave vector, at walls of arbitrary scattering properties. (The values of the wall roughness ρ in the previous report[11] were given divided by a factor of 2, i.e., they should be multiplied by that factor in order for them to correspond to the figure of that paper. Similarly, the stated values of the alternative measure of roughness p,[12]

$$p=1-4\int_0^{\pi/2} d\theta\cos\theta\sin^3\theta\exp(-2\rho/\cos\theta) \tag{1.1}$$

should be changed into $p=0.0$, 0.095, 0.358, 0.562, 0.998.)

The probability of Andreev reflection, and all other coefficients of various branch conversion processes, depends on the quasiparticle energy and the incident angle of approach into the wall region in addition to the roughness of the surface and the temperature. It is clear that there is no way of sensibly presenting an exhaustive account of all the conceivable branch conversions and other processes. In order to cut down on the number of coefficients to be calculated, we always consider an incident nonmagnetic particlelike excitation. One just needs this (and the completely equivalent holelike nonmagnetic initial excitation result) for the hydrodynamic slip length, for example.

Section II is a summary of the theory of scattering of an excitation off a rough surface. The relatively involved numerical calculations are discussed in detail. In Sec. III, plots of the conversion coefficients are discussed in a set of illustrative cases. These consist of the energy dependence of the different coefficients at given incident angles and given surface roughnesses at a given temperature, as well as of the angular dependence at a given energy and several roughnesses. There are a number of plots of the amplitudes of the diffuse background scattering as well. There is finally a short discussion of the results.

II. THEORY AND CALCULATIONS

The theoretical framework used here is the quasiclassical approach to superfluid ^{3}He as reviewed by Serene and Rainer.[5] Their notation is essentially used throughout.

Diffuse scattering of quasiparticles at a wall would normally be an unpleasantly complicated boundary condition on the quasiclassical Green's functions.[13] That problem is taken care of with a model of Ovchinnikov[14] slightly generalized by Culetto *et al.*[15] where a specularly reflecting wall is thought to be covered with a thin layer of dirt providing the diffuse scattering. The thickness of the layer d and its scattering mean free path l are imagined to be very small compared to the coherence length, in which case the thickness becomes an irrelevant parameter and the roughness of the wall is determined by the ration $\rho=d/l$.

We basically need solutions to the transportlike equation for the Keldysh propagator $\hat{g}^K(\hat{\mathbf{k}},\mathbf{R};\varepsilon)$. In order to incorporate the diffuse scattering we also need the same function in the scattering layer where we call it $\hat{\gamma}^K$. The two have to be matched at the surface between the ^{3}He and the scattering layer. The boundary condition for $\hat{\gamma}^K$ behind the scattering layer is taken to be specular. In the helium region, the equation for $\hat{g}^K$ reads

$$[\varepsilon\hat{\tau}_3-\hat{\Delta},\hat{g}^K]_-+iv_F\hat{\mathbf{k}}\cdot\nabla_{\mathbf{R}}\hat{g}^K=0\ . \tag{2.1}$$

The matrix $\hat{\Delta}$ is the order parameter previously determined self-consistently.[11] In homogeneous ^{3}He, the 16 basic solutions of eq. (2.1) are the excitations referred to in the Introduction. Actual quasiparticles, packets of excitations, can be constructed out of these.[1] In the scattering layer, the scattering is so strong as to drown all other sources of self-energy and the commutator $[\varepsilon\hat{\tau}_3,\hat{g}^K]$. The self-consistent Born approximation is taken for the advanced, retarded, and Keldysh self-energies resulting in

$$\frac{2\pi i}{\rho}k_\perp\frac{d}{d\xi}\hat{\gamma}^K+\hat{\gamma}^R\langle\hat{\gamma}^K\rangle+\hat{\gamma}^K\langle\hat{\gamma}^A\rangle-\langle\hat{\gamma}^R\rangle\hat{\gamma}^K-\langle\hat{\gamma}^K\rangle\hat{\gamma}^A=0 \tag{2.2}$$

for the Keldysh propagator in the scattering layer. The propagator depends only on the scaled distance $\xi=z/d$. The dot product between $\hat{\mathbf{k}}$ and the gradient operator is thus replaced by $k_\perp d/d\xi$. The superscripts A and R denote the advanced and retarded propagators, and the angular brackets stand for an average over the Fermi sphere with respect to $\hat{\mathbf{k}}$.

Outside the scattering layer, the retarded and advanced functions obey the same differential equation as $\hat{g}^K$. This, of course, is the same equation as obeyed by the Matsubara Green's function when the latter is interpreted as being taken at an energy approaching the real axis from above or from below, $i\varepsilon_n\to\varepsilon\pm0^+$. All the equations are identical because the order parameter $\hat{\Delta}$ is analytic across the real axis which implies $\hat{\Delta}^A=\hat{\Delta}^R=\hat{\Delta}$. Although the retarded and advanced Green's functions are not needed in the equation for the Keldysh propagators in the ^{3}He, they are required in the scattering layer, as can be seen in Eq. (2.2). There they obey the equation

$$\frac{2\pi i}{\rho}k_\perp\frac{d}{d\xi}\hat{\gamma}^{R,A}+[\hat{\gamma}^{R,A},\langle\hat{\gamma}^{R,A}\rangle]_-=0\ . \tag{2.3}$$

Obviously $\hat{g}^R$ and $\hat{g}^A$ have to be calculated in the ^{3}He as well, in order to establish them in the scattering layer. Asymptotic values for them in bulk ^{3}He are given in the review article of Serene and Rainer.[5] They obey the normalization condition

$$[\hat{g}^{R,A}(\hat{\mathbf{k}},\mathbf{R},\varepsilon)]^2=-\pi^2\ , \tag{2.4}$$

and the boundary condition on the outside wall

$$\hat{\gamma}^{R,A,K}(-k_\perp,0,\varepsilon)=\hat{\gamma}^{R,A,K}(k_\perp,0,\varepsilon)\ , \tag{2.5}$$

and their numerical calculation is routine. Actually only one of them needs to be calculated because of the symmetry relation

$$\hat{g}^A=\hat{\tau}_3(\hat{g}^R)^+\hat{\tau}_3\ . \tag{2.6}$$

The final step is finding the Keldysh Green's function.

Here the problem splits into two stages. The incident and specularly scattered rays can be treated separately from the background scattering continuously distributed in $\hat{\mathbf{k}}$. An incident unit amplitude "plane wave" of quasiparticles in some direction $\hat{\mathbf{k}}^p$ is considered. A complete trajectory, including the collision with the wall, consists of the initial branch and the branch specularly transmitted at the wall. The incident ray trajectory and its mirror reflected partner, the "principal rays" are a special pair in the present problem. They each have an infinitely large weight compared with any one $\hat{\mathbf{k}}$ background scattered ray. Therefore, only two self-energy terms of Eq. (2.2) have to be included for them. The result is the simpler equation

$$\frac{2\pi i}{\rho} k_\perp \frac{d}{d\xi} \hat{\gamma}^K + \hat{\gamma}^K \langle \hat{\gamma}^A \rangle - \langle \hat{\gamma}^R \rangle \hat{\gamma}^K = 0 . \tag{2.7}$$

The final state will consist of a number of excitations along the initial trajectory and along the transmitted trajectory. One expects part of the incident wave to be Andreev reflected into any of the four possible holelike states that propagate backward in $\hat{\mathbf{k}}$. The presence of excitations propagating in opposite directions, furthermore, calls for the presence of Tomasch solutions on the initial branch of the trajectory. On the trajectory transmitted at the wall, there should be no excitations running toward the wall in the asymptotic region far from the wall. There should, therefore, be no Tomasch interferences either. This leaves four possible particlelike modes propagating outward. There are thus 16 asymptotic amplitudes to be fixed altogether, four plus eight on the initial branch of the trajectory and four on the transmitted part. This can be accomplished using the 16 conditions of specular reflection at the wall behind the scattering layer (2.5). The amplitudes are directly the Andreev reflection and transmission plus branch conversion coefficients relating to an incoming particlelike excitation.

There are two aspects worth mentioning about the background calculation. The first one is the self-consistency problem in the source terms of Eq. (2.2) that were not present in the principal ray calculation. These terms feature the angular average of $\hat{g}^K$ in which there are contributions from the principal ray and the background solution itself. The latter input must be determined self-consistently. For this purpose it looks like a fruitful strategy to compute, instead of each trajectory separately, a global solution of the linear simultaneous equations of all the trajectories thus automatically taking care of the self-consistency. As a cost of the simplification, the dimensionality of the differential equation becomes multiplied by the number of points of the (Gaussian) integration of the trajectory wave vector over the Fermi surface.

The second noteworthy feature of the background problem is that it appears overdetermined. Intuitively there shall be only outgoing excitations in the background scattering and, therefore, no Tomasch interferences either. On each specularly reflected pair of rays there are thus altogether eight free amplitudes at our disposal, those of four holes on the part of the trajectory with $\hat{\mathbf{k}}$ pointing into the wall and those of four particles on the outward half, and this should be suffice to satisfy the 16 conditions of specular reflection at the wall. It is the normalization condition of the theory that guarantees the existence of this kind of a solution. The normalization condition for the Keldysh Green's function $\hat{g}^K(\hat{\mathbf{k}}, \mathbf{R}, \varepsilon)$ reads

$$\hat{g}^R \hat{g}^K + \hat{g}^K \hat{g}^A = 0 . \tag{2.8}$$

The normalization is conserved by all the quasiclassical equations of motion. We can demand it in the far region into the bulk where the asymptotic nature of the solutions is clear. All the different Green's functions are analytically known in bulk ^{3}He where the order parameter is a constant. We know that the advanced and retarded Green's functions are linear combinations of the analytic continuations of physical constant Matsubara Green's functions and two components which decay into the bulk. We used the symbolic expressions manipulating program Macsyma to calculate the normalization expressions between the various asymptotic Keldysh Green's functions propagating into the fluid and the three conceivable components of the advanced and retarded functions. All of the 24 conditions were individually satisfied. This implies that the outgoing solutions can exist without the presence of either incoming or Tomasch solutions. If the normalization expressions are calculated for either of the latter two with the retarded and advance functions "decaying" into the bulk, it is found that only a linear combination of incoming and Tomasch solutions can meet the normalization condition, neither kind of the two alone. The upshot is that the Tomasch amplitudes are fixed by the incoming solutions alone although they superficially look like they are interferences of the incoming and outgoing solutions. We, therefore, know that a background solution exists which consists only of outgoing solutions. In the practical computation, the amplitudes of the outgoing solutions were simultaneously optimized for all the background trajectories. Minimum square deviation from a 16-amplitude specular match per trajectory at the outside wall of the scattering layer was sought. The match was perfect within numerical accuracy.

The various transmission and reflection coefficients are defined as ratios of the corresponding amplitudes to the incoming amplitude. Following Kieselmann *et al.*[1] we assign two subscripts to the transmission coefficient T_{ij} and the reflection coefficient R_{ij}. The first of these subscripts refers to the nonmagnetic (0) or magnetic (1–3) quality of the initial ray, and the latter to the transmitted or the reflected ray. Because of the particle-hole symmetry, it does not matter for the numerical values of the various coefficients whether the initial ray is particles or holes. We extend the symbol R_{on} to refer to the excitations (holes in the present numerical calculation) running away from the wall on a background trajectory pointing toward the wall. The conservation of the number of excitations requires

$$\sum_{\hat{\mathbf{k}}_{in}} |\hat{\mathbf{n}}\cdot\hat{\mathbf{k}}_{in}| R_{oo}(\hat{\mathbf{k}}_{in},\hat{\mathbf{k}}^p,\varepsilon)+\sum_{\hat{\mathbf{k}}_{out}} |\hat{\mathbf{n}}\cdot\hat{\mathbf{k}}_{out}| T_{oo}(\hat{\mathbf{k}}_{out},\hat{\mathbf{k}}^p,\varepsilon)=|\hat{\mathbf{n}}\cdot\hat{\mathbf{k}}^p|(1-T_{oo}^p-R_{oo}^p)\ , \tag{2.9}$$

where the sums run over the unit wave vectors pointing into and out of the wall, respectively, $\hat{\mathbf{n}}$ is the normal to the wall, and the superscript p distinguishes the principal ray from the rest. In the absence of background scattering, Eq. (2.9) reduces to the simpler form[1]

$$R_{oo}^p+T_{oo}^p=1\ . \tag{2.10}$$

The conservation of the number of excitations is not the same as the conservation of physical particles. The number of physical particles (or holes, for that matter) is not conserved in the scattering unless collective degrees of freedom are kept track of.

III. RESULTS

In our first set of figures, Figs. 1(a)–1(c), the various Andreev conversion coefficients along the principal rays are plotted as functions of the incident angle with respect to the plane of the wall. The temperature is chosen as $T=0.3T_c$ and the incident energy as $\varepsilon=1.098$, as mea-

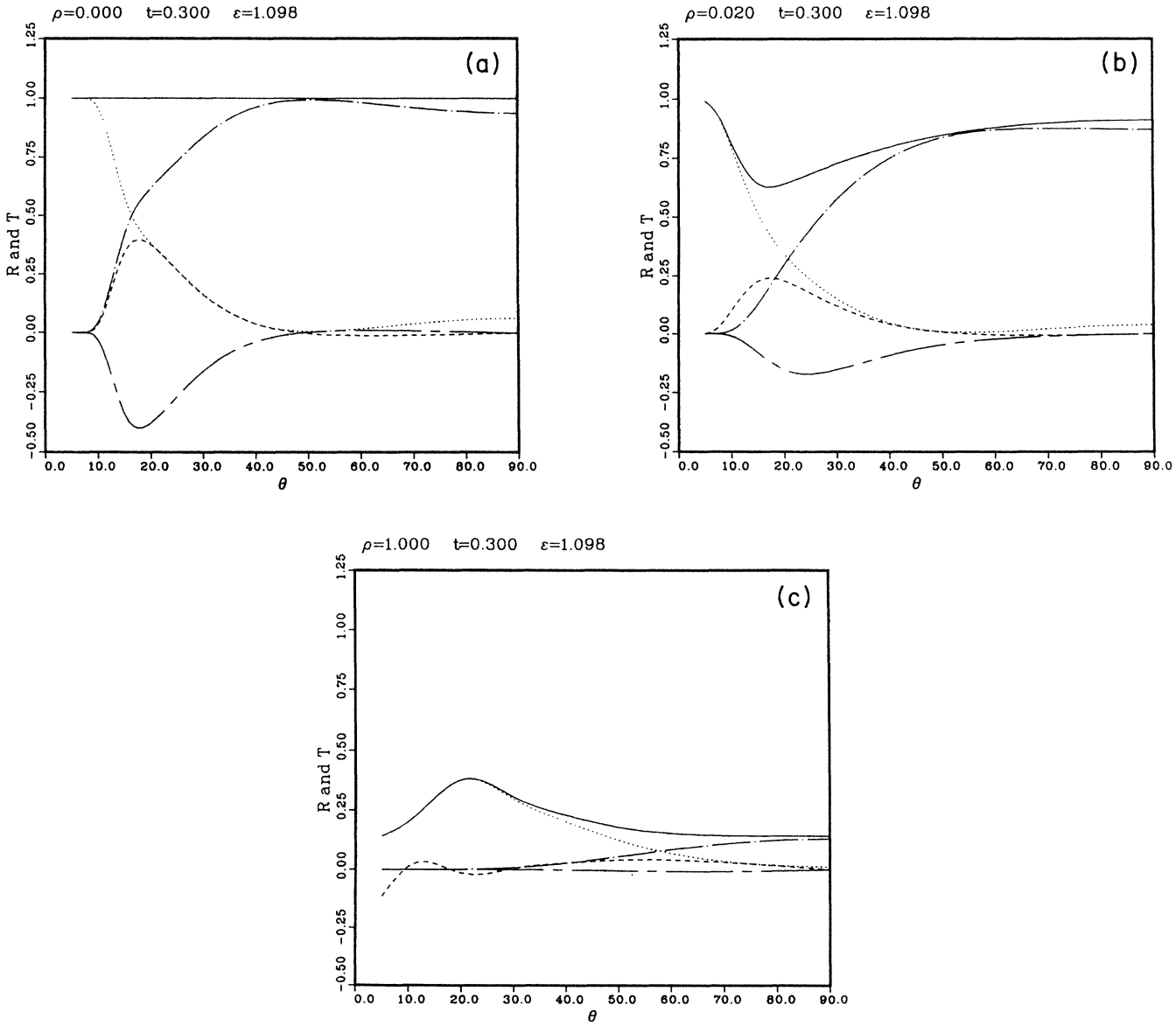

FIG. 1. Andreev transmission and reflection coefficients as functions of the incident angle relative to the plane of the wall. Dotted line R_{oo}, dashed line R_{on}, short-dashed line T_{oo}, long-dashed line T_{on}. The solid line is the sum of $R_{oo}+T_{oo}$. All plots are at incident particle energy $\varepsilon=1.098$, reduced temperature $t=0.3$, and at the roughnesses ρ of the wall, $\rho=0$ in (a) 0.02 in (b), and 1.0 in (c).

sured in units of the bulk gap. Figure 1(a) plays the role of a point of comparison displaying the specular scattering result. Figures 1(b) and 1(c) show the effect of diffuse scattering of quasiparticles at two different roughnesses of the wall, $\rho=0.02$ and 1.00. In addition to the coefficients R_{oo} and T_{oo} and their sum, we plot the coefficients R_{on} and T_{on} which carry information about the conversion rate of the unpolarized initial beam into spin-polarized reflected or transmitted states.[1] The subscript n of R_{on} or T_{on} points to the spin-polarization direction of a magnetic excitation. It turns out that only one magnetic branch is excited in the principal beam. Its magnetization is parallel to the wall and perpendicular to the incident $\hat{\mathbf{k}}$, if the B-phase rotation matrix is chosen to be the unit matrix. If (say the energy minimizing) rotation around the perpendicular direction to the wall is taken into account, the magnetic branch still has its magnetization parallel to the wall but now perpendicular to the spin direction rotated away from the initial $\hat{\mathbf{k}}$ direction. With specular scattering, Fig. 1(a) the simple sum rule (2.10) is obeyed and R_{on} and T_{on} are symmetrical about the value zero. When diffusive scattering sets in, Figs. 1(b) and 1(c), the sum simple rule (2.10) becomes violated to a degree which depends on the angle. The symmetry of R_{on} and T_{on} is then destroyed.

Irrespective of the symmetry between R_{on} and T_{on}, magnetization is transported into the fluid. The missing magnetization must go into some kind of collective excitations which should be an observable effect.[1] By the time the roughness has reached the value $\rho=1$, most of the scattering is diffuse and there is practically no transmitted wave or conversion into magnetic branches.

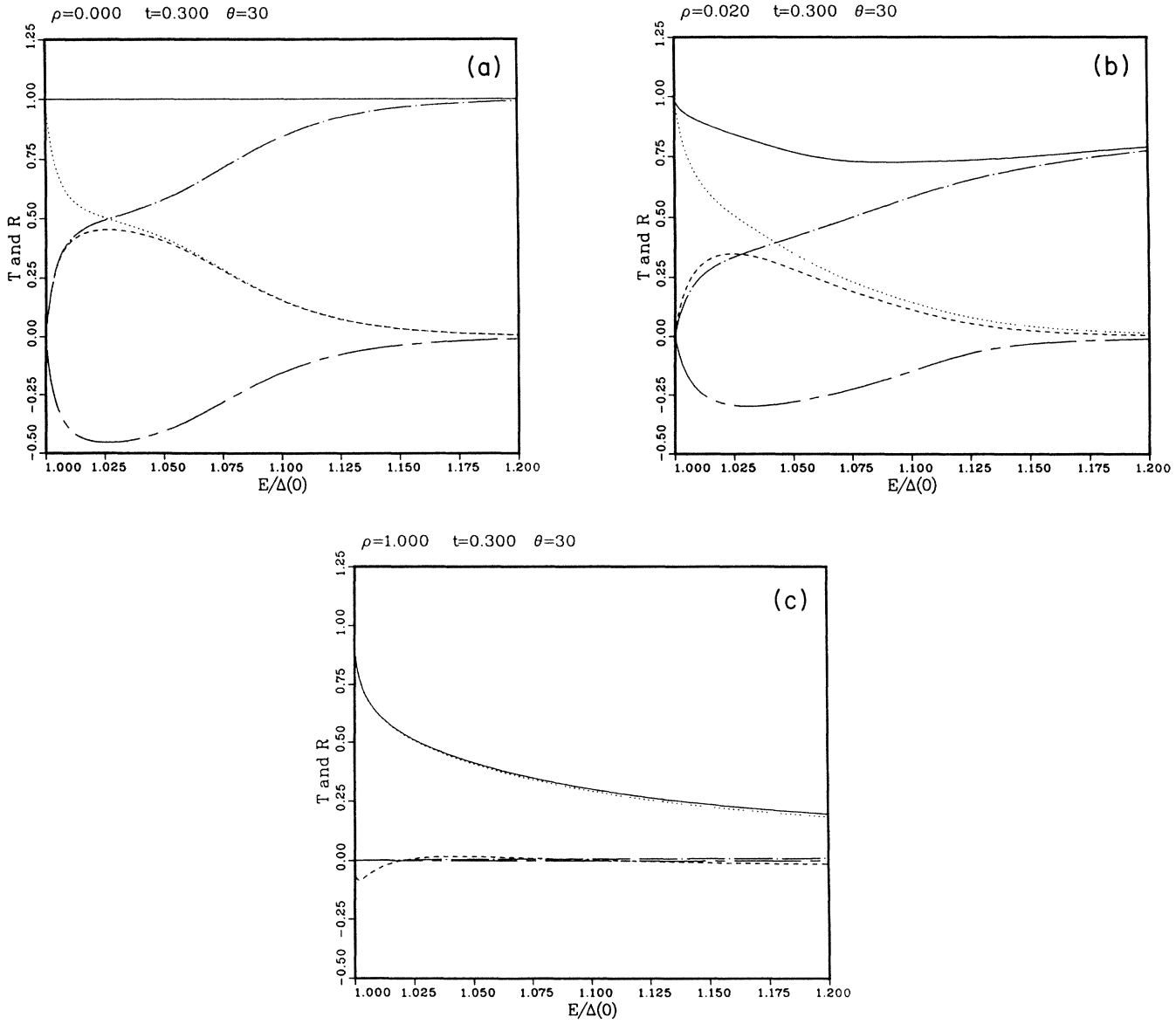

FIG. 2. The Andreev transmission and reflection coefficients as functions of the incident energy at the incident angle $\theta=30°$ and at the reduced temperature $t=0.3$. The different lines are the same as in Fig. 1. The different roughnesses are also the same as in Fig. 1.

One also observes that scattering into magnetic states mostly takes place at glancing angles and is no more present at perpendicular incidence. Another observation, not in conflict with our intuition, is the vanishing of the transmission coefficient at all at glancing incidence at energies near the bulk gap edge.

The next triplet of pictures, Figs. 2(a)–2(c), are analogous to the above but now at a fixed angle of scattering, $\theta = 30°$, as a function of the initial energy of the incoming beam. Again there is symmetry of the magnetic conversion in the case of specular scattering which is broken when diffusivity sets in. It is intuitively pleasing to notice that the reflection coefficient is high at small energies. In the roughest case, all coefficients, apart from the simple Andreev reflection, are small at all energies. Figures 3(a)–3(c) are the same as Figs. 2(a)–2(c) but at perpendicular incidence. There is no magnetic conversion, and the transmission coefficient saturates at high energies at a value which is a function of ρ. At the same time, the reflection coefficient becomes an ever steeper function of the energy vanishing already at quite small energies at high values of ρ.

Four figures, 4(a), 4(b), 5(a), and 5(b) display the background scattering coefficients at two different roughnesses of the wall with two different angles of incidence of the incoming ray in both. In order to keep the amount of information within bounds, only the nonmagnetic, i.e., total amplitudes are given; they have not been analyzed into the different magnetic components. In all figures, the transmission coefficients are given as functions of the energy (scaled to the bulk gap). As defined above, the symbol T is used for particles along outgoing wave vectors and the symbol R for holes outward along incoming wave vectors. The two are plotted with identical lines in all the

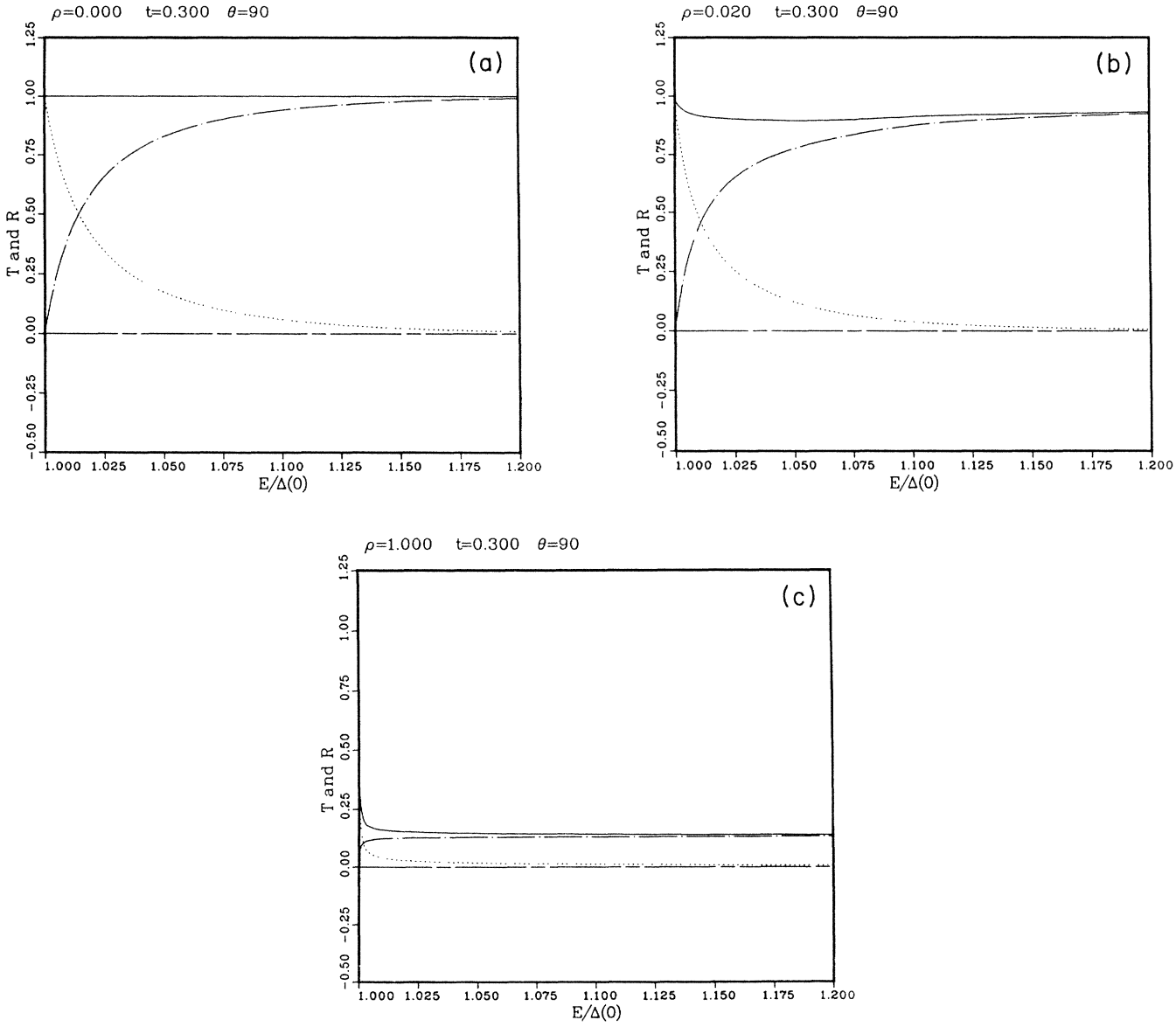

FIG. 3. Same as in Fig. 2 but at the incident angle $\theta = 90$, i.e., normal incidence. There is no magnetic conversion present.

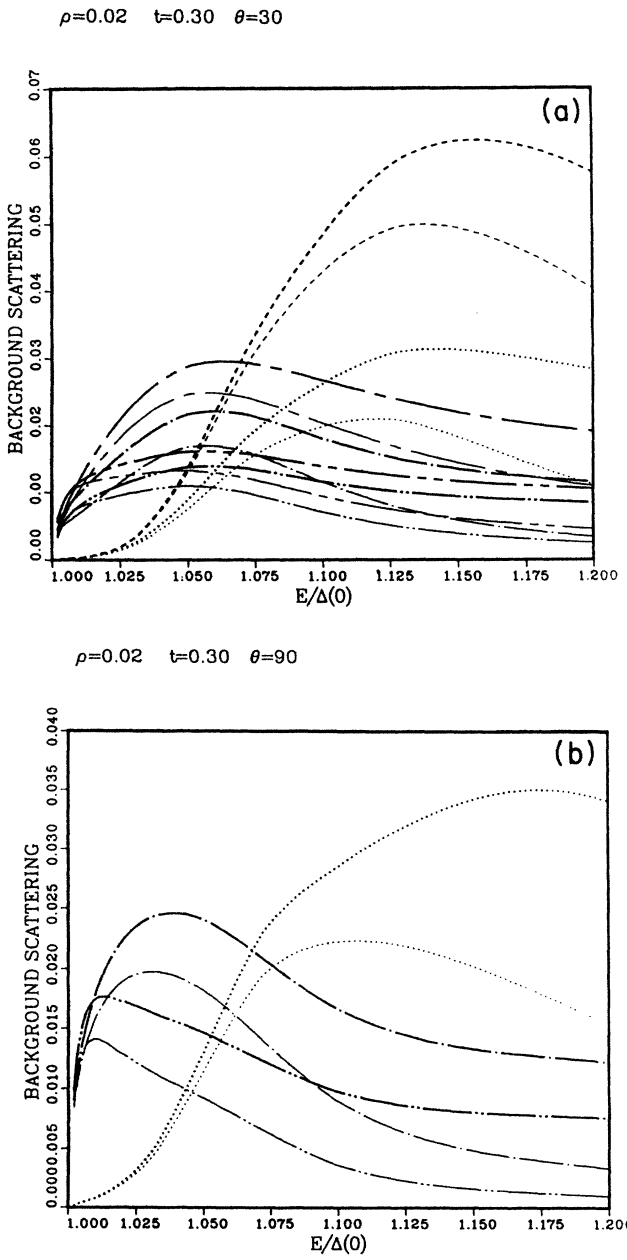

FIG. 4. The diffuse background scattering at $\rho=0.02$ and temperature $t=0.3$, (a) with the polar angle of the principal ray as measured from the plane of the wall $\theta=30°$, and (b) with $\theta=90°$, i.e., at normal incidence. Each picture displays the background scattering on trajectories with their outward halves at three difference polar angles measured from the plane of the wall and two different azimuthal angles as measured from the forward direction of the principal ray. Line thickness differentiates between particles and holes. Particles, symbolized by thick lines, depart forward along the trajectory, and holes, symbolized by thin lines, backward on the incoming half, i.e., actually at azimuthal angles of the particles plus π. Dots on a line dedicate it to a trajectory with the azimuthal angle $\phi=25°$, dashes with the angle $\phi=119°$. The third dimension of line variation fixed the polar angles. Simple dots or dashes mean $\theta=14°$, a short dashed or long dashed $\theta=41°$, and double dotted or double dashed $\theta=69°$. The difference between a dashed line and a dotted line reflects the azimuthal asymmetry of the scattering. At perpendicular incidence there is no asymmetry.

figures, only thicker for particles and thinner for holes. The computations were carried out for three polar angles $\theta=14°$, 41°, and 69° measured from the plane of the wall and two azimuthal angles $\phi=25°$ and 119° (24 Gauss points, i.e., 12 mirror reflecting pairs of rays). Lines in two of the lower-roughness figures come in pairs reflecting the asymmetry of the azimuthal distribution, the higher amplitude being for $\phi=119°$. This asymmetry obviously dissolves at perpendicular incidence, and it is so small as to be indistinguishable on the scale of the

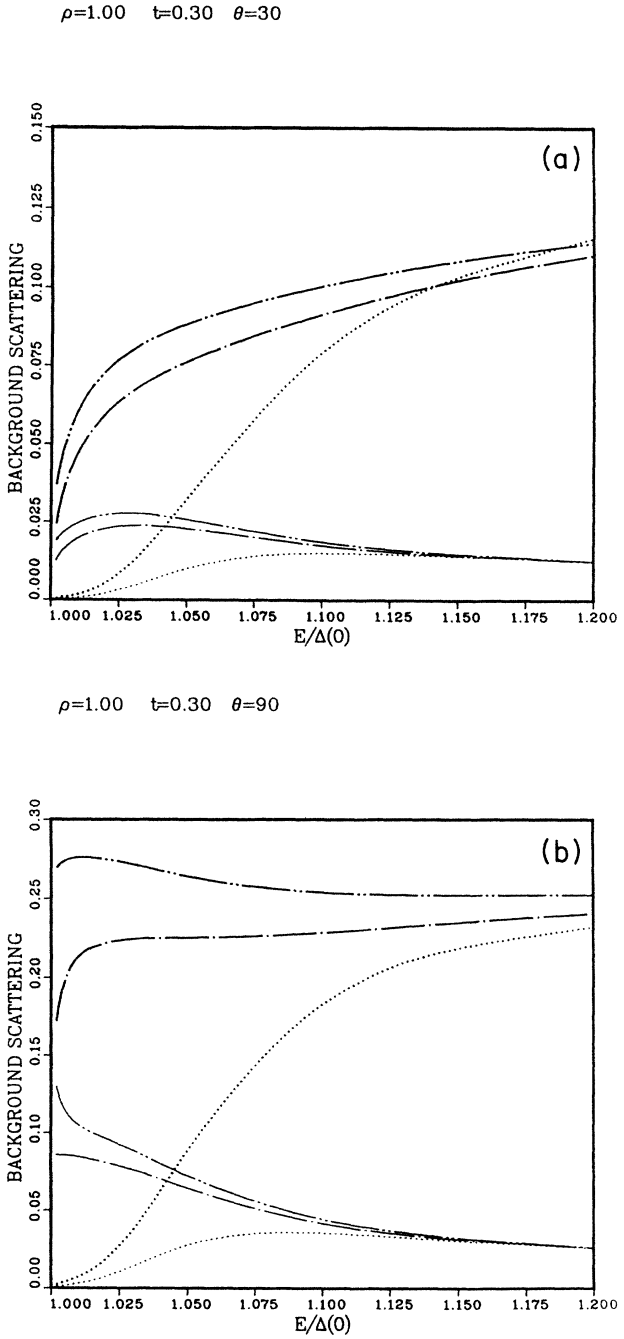

FIG. 5. Same as above at $\rho=1$. The essential differences as compared to Figs. 4(a)–4(c) are the different scales of the plotted coefficients and the absence of azimuthal asymmetry.

figures at $\rho=1$. It should be noticed that the scales are different in the two sets of figures at different roughnesses because of the higher total intensity of the background with the more diffusely scattering surface.

IV. DISCUSSION

We have calculated the fate of a particlelike excitation of ^{3}He when it meets a diffusely scattering wall. We chose the rather low temperature $t=0.3$ since the question studied gains in experimental significance at low temperatures.

As explained in the Introduction, there is an enormous amount of information in the various magnetic and nonmagnetic amplitudes as functions of the incident beam energy and direction, the roughness of the wall, and the temperature. The set of figures is an attempt to give an overall impression of the wealth of phenomena going on. The whole information can be translated into fairly compact form by computing hydrodynamic slip lengths and viscosities in the ballistic regime,[16,7] for instance, to which we will return in a later publication.

The general features of the results are not in conflict with our intuition. For example, the amplitude of the specularly transmitted ray diminishes rapidly when the diffusivity of the surface increases and an increasing share of the scattered excitations go into a diffuse background scattering. At lowish diffusivities of the wall, the diffuse scattering is backward weighted for particlelike excitations and forward weighted for holelike excitations but becomes azimuthally symmetric when the wall becomes very rough. The momentum transport to the wall is mainly determined by the portion of the incident ray which is diffusely scattered; the integrated parallel momentum of the background scattering is small, but backward weighted, at all roughnesses. This may be an artifact of the thin-dirty-layer model of a diffusely scattering surface.

ACKNOWLEDGMENT

One of us (J.K.) thanks the Finnish Academy for financial support.

[1]G. Kieselmann and D. Rainer, Z. Phys. B **52**, 267 (1983).
[2]A. F. Andreev, Zh. Eksp. Teor. Fiz. **46**, 1823 (1964) [Sov. Phys.—(JETP) **19**, 1228 (1964)].
[3]V. Ambegaokar, P. G. deGennes, and D. Rainer, Phys. Rev. A **9**, 2676 (1974).
[4]L. J. Buchholtz and G. Zwicknagl, Phys. Rev. B **23**, 5788 (1981).
[5]J. W. Serene and D. Rainer, Phys. Rep. **101**, 221 (1983).
[6]N. A. Greaves and A. J. Leggett, J. Phys. C **16**, 4383 (1983).
[7]H. Hojgaard Jensen, H. Smith, P. Wölfle, K. Nagai, and T. M. Bisgaard, J. Low Temp. Phys. **41**, 473 (1980).
[8]D. Einzel, P. Wölfle, H. Hojgaard Jensen, and H. Smith, Phys. Rev. Lett. **52**, 1705 (1984).
[9]A. Kundt and E. Warburg, Ann. Phys. (Leipzig) **155**, 337 (1875).
[10]C. N. Archie, T. A. Alvesalo, J. D. Reppy, and R. C. Richardson, J. Low Temp. Phys. **42**, 295 (1980).
[11]Weiyi Zhang, J. Kurkijärvi, and E. V. Thuneberg, Phys. Lett. **109A**, 238 (1985).
[12]G. Lüders and K. D. Usadel, Vol. 56 of *Springer Tracts in Modern Physics* (Springer-Verlag, Berlin, 1971).
[13]L. J. Buccholtz and D. Rainer, Z. Phys. B **35**, 151 (1979).
[14]Yu. N. Ovchinnikov, Zh. Eksp. Teor. Fiz. **56**, 1580 (1969) [Sov. Phys.—(JETP) **29**, 849 (1969)].
[15]F. J. Culetto, G. Kieselmann, and D. Rainer, in *17th International Conference on Low Temperature Physics, LT-17,* edited by U. Eckern, A. Schmid, W. Weber, and H. Wühl (North-Holland, Amsterdam, 1984), p. 1027.
[16]D. Einzel, H. Hojgaard Jensen, H. Smith, and P. Wölfle, J. Low Temp. Phys. **53**, 695 (1983).